

## Charmed Hadrons from Fragmentation and $B$ Decays

Jens Sören Lange, for the Belle Collaboration

*Johann Wolfgang Goethe-Universität, Institut für Kernphysik,  
Max-von-Laue-Straße 1, D-60438 Frankfurt am Main*

The fragmentation functions of  $D^0$ ,  $D^\pm$ ,  $D_s^\pm$ ,  $D^{*0}$ ,  $D^{*\pm}$  and  $\Lambda_c^\pm$  at  $\sqrt{s}\simeq 10.6$  GeV are measured with a data set of  $102.7\text{ fb}^{-1}$ . Fragmentation model parametrizations (Peterson, Kartvelishvili, Collins-Spiller, Lund, and Bowler models) are compared to the data. The data at high  $x\simeq 1$  indicate a contribution of non-perturbative QCD processes.

*Keywords:* QCD; Fragmentation; Charm Quarks.

PACS numbers: 13.66.Bc, 13.87.Fh, 14.40.Lb

### 1. Introduction

The Belle experiment<sup>1</sup> at the asymmetric  $e^+e^-$  collider<sup>2</sup> KEK-B in Tsukuba, Japan, is operating with an  $e^-$  beam energy of 8.0 GeV and an  $e^+$  beam energy of 3.5 GeV. The center-of-mass (cms) energy is adjusted to a  $\sqrt{s}=10.58$  GeV, corresponding to the mass of the  $\Upsilon(4S)$  resonance. At this cms energy, there is a resonant and a non-resonant component: the resonant  $\Upsilon(4S)$  is produced with a cross section of  $\sigma\simeq 1.2$  nb, the non-resonant continuum with  $\sigma\simeq 3.0$  nb. The  $\Upsilon(4S)$  decays into  $B\bar{B}$  meson pairs with a branching fraction higher than 99%, and  $\simeq 99\%$  of all  $B(\bar{B})$  mesons decay into final states with hadrons containing charm quarks. In the continuum, the cross section of direct charm production is also high, i.e.  $\sigma\simeq 1.3$  nb. For about 10% of the time, data are recorded at  $\sqrt{s}=10.52$  GeV, containing only the non-resonant continuum component.

Fragmentation is a QCD process which involves not only single partons, but a cascade of many partons, as it is shown schematically in Fig. 1. A single bare charm quark starts radiating gluons. The gluons themselves may a.) radiate additional gluons directly, or b.) convert into  $u\bar{u}$ ,  $d\bar{d}$  or  $s\bar{s}$  quark-antiquark pairs, while those quarks then might radiate additional gluons. If the distances between the quarks become too large ( $r\geq 1$  fm), hadronisation starts and final state mesons and baryons are generated.

The study of fragmentation has two aspects: On the one hand, as a theoretical aspect, QCD predicts hadronic confinement, but does not predict how an initial state quark as a pointlike object transforms into a final state hadron, i.e. an confined object with a formfactor. In most fragmentation models, the splitting of one

\*Present Address: Justus-Liebig-Universität Gießen, II. Physikalisches Institut, Heinrich-Buff-Ring 14, 35392 Gießen, Email Soeren.Lange@physik.uni-giessen.de

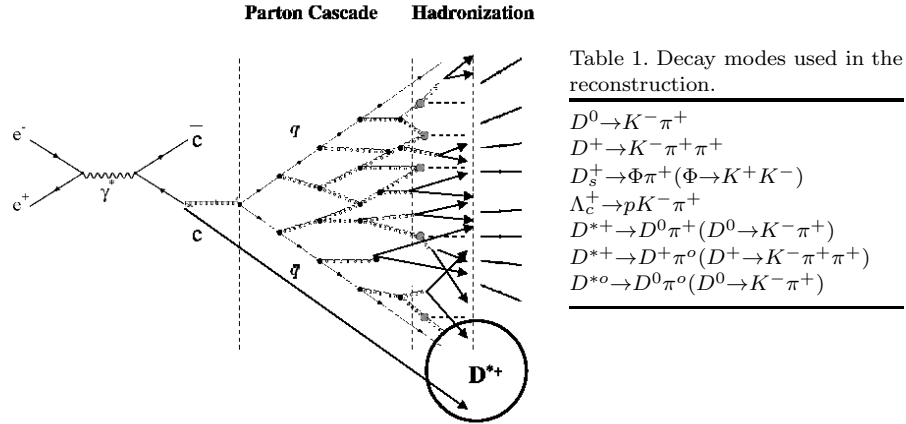


Table 1. Decay modes used in the reconstruction.

$D^0 \rightarrow K^- \pi^+$
$D^+ \rightarrow K^- \pi^+ \pi^+$
$D_s^+ \rightarrow \Phi \pi^+ (\Phi \rightarrow K^+ K^-)$
$\Lambda_c^+ \rightarrow p K^- \pi^+$
$D^{*+} \rightarrow D^0 \pi^+ (D^0 \rightarrow K^- \pi^+)$
$D^{*+} \rightarrow D^+ \pi^0 (D^+ \rightarrow K^- \pi^+ \pi^+)$
$D^{*0} \rightarrow D^0 \pi^0 (D^0 \rightarrow K^- \pi^+)$

 Fig. 1. Schematic description of the process  $e^+e^- \rightarrow c\bar{c}$  with subsequent fragmentation of the charm quark into a  $D^*$ .

parton to many partons (the ‘‘parton shower’’) is treated in perturbative QCD only, and hadronisation models are only phenomenological with minor predicting capabilities. Heavy quarks are in particular of interest, because their production is strongly suppressed in both the parton shower and the hadronisation. Thus, a final state charmed hadron contains a charm quark, which was produced with a high probability in the primary interaction.

On the other hand, as a practical aspect, it is important to improve Monte-Carlo (MC) event generators. Several other analyses of direct charm production e.g. production of  $D^{**}$ ,  $D_{s,J}$  etc. require MC simulations of charm fragmentation. In this paper PYTHIA<sup>5</sup> 6.2 is used. The event generators use parameters, which have to be constrained by comparison to experimental data.

The relevant variable for the investigation of the process dynamics is the momentum fraction  $x = p_{hadron}/p_{quark}$ . As the quark momentum is a priori unknown and can only be approximated, in this paper  $x_p = p/p_{max}$  is used, where  $p_{max}$  is corrected for the mass of the final state hadron, i.e.  $p_{max} = \sqrt{s/4 - m_{hadron}^2}$ . The fragmentation function  $D(x_p)$  is then given as the normalized yield as a function of  $x_p$ . Instead of the yield, related quantities such as the cross section  $d\sigma/dx_p$  or  $BR \times d\sigma/dx_p$  can be used, where BR denotes the branching ratio into the particular final state. For the functional form of fragmentation functions, in PYTHIA the variable  $z$  is used instead of the variable  $x_p$ , which is defined as  $z = (E + p_z)_{hadron}/(E + p_z)_{quark}$ .

As will be shown below, in particular the high  $x$  region (i.e.  $x_p \simeq 1$  or  $z \simeq 1$ ) might be sensitive to effects of non-perturbative QCD. The  $x=1$  limit is corresponding to the exclusive process e.g.  $e^+e^- \rightarrow c\bar{c} \rightarrow D^0 \bar{D}^0$ , in which on either side a bare charm quarks transforms into a hadron, which contains the identical charm quark as a valence quark, but additionally one light valence quark, light sea quarks and sea gluons. The interesting aspect is that, due to  $p_{hadron} = p_{quark}$ , no momentum is

available to create the hadronic structure, but in fact the momentum balance is provided by the QCD vacuum.

Fragmentation data of  $e^+e^- \rightarrow c\bar{c}$  at  $\sqrt{s} \simeq 10.6$  GeV have been measured previously, but with lower statistical significance. More than 10 years ago, the ARGUS collaboration and the CLEO collaboration published<sup>8,9</sup> data based upon integrated luminosities of  $31.4 \text{ pb}^{-1}$  and  $35.8 \text{ pb}^{-1}$ , respectively. Nowadays, equivalent data are recorded by BELLE in  $\simeq 50$  minutes. More recently, the CLEO collaboration published<sup>10</sup>  $D$  and  $D^*$  fragmentation data based upon  $8.9 \text{ fb}^{-1}$ .  $D_s$  and  $D_s^*$  fragmentation data were published<sup>11,12</sup> by CLEO and by BABAR based upon  $4.7 \text{ fb}^{-1}$  and  $23.4 \text{ fb}^{-1}$ , respectively.

## 2. Analysis

A data set of  $87.7 \text{ fb}^{-1}$  on-resonance and  $15.0 \text{ fb}^{-1}$  off-resonance is used, and compared to Monte Carlo (MC) simulations corresponding to  $217.0 \text{ fb}^{-1}$ . The MC simulations are based upon the event generator QQ98<sup>3</sup> for  $e^+e^- \rightarrow c\bar{c}$ , the Peterson<sup>4</sup> fragmentation model, PYTHIA<sup>5</sup> 6.2 for the parton shower evolution and GEANT<sup>6</sup> 3.21 for the detector description. For specific simulations, also different fragmentation models are used (see below). The decay modes used in the reconstruction are listed in Tab. 1. Charge conjugated modes are included. The efficiencies for particle identification of  $\pi^\pm$  and  $K^\pm$  are above 96% for all decay modes, the efficiency for protons is 81%. The particle misidentification probabilities are between 12% and 26%. This paper represents a short version of the complete analysis which is published elsewhere<sup>7</sup>. With this unprecedented statistics it became possible to reduce the bin width in  $x_p$  by a factor of  $\simeq 3$ , and thus investigate the shape of the fragmentation function with high precision, in particular in the high  $x_p \simeq 1$  region. In addition, fragmentation into the baryon  $\Lambda_c$  is measured, for which a high statistics data set has not been available previously.

Fig. 2 shows the mass distribution<sup>a</sup> for the  $D^0$  and the  $\Lambda_c^+$  (as an example for the meson and baryon reconstruction). The signals are shown for a momentum fraction  $0.68 < x_p < 0.70$ , which is close to the  $x_p$  of peak position in the fragmentation function. The cross sections are calculated using the fitted signal yields.

As mentioned above, at  $\sqrt{s} = 10.6$  GeV there is a resonant and a non-resonant contribution. Thus, charmed hadrons can be produced by  $B$  decays (whereas the  $B$  mesons are produced by decay of the  $\Upsilon(4S)$  resonance) or by fragmentation. In a first step, these two contributions have to be identified. Fig. 3 shows the cross section  $d\sigma/dx_p$  as a function of  $x_p$ . The down-left hatched histogram shows on-resonance data, the down-right hatched histogram shows off-resonance data. After normalisation using the integrated luminosities of the respective samples, the naive  $1/s$  dependence on the total hadronic cross section has been taken into account by a weighting factor  $(10.58 \text{ GeV}/10.52 \text{ GeV})^2$ . The contribution of  $B$  decays is

<sup>a</sup>The mass distributions in Fig. 2 are shown as mass difference distributions of the measured mass and the mass as given by the PDG<sup>13</sup>.

dominant at lower  $x_p < 0.5$ , as the  $B$  decay kinematics limits the maximum possible momentum of the charmed hadron to about  $p_{hadron} \simeq 2.5$  GeV/c, corresponding to  $x_p \simeq 0.5$ . The distributions in Fig. 3 are not yet efficiency corrected and only statistical errors are shown.

### 3. Fragmentation Functions

Fig. 4 shows the cross section  $d\sigma/dx_p$  as a function of  $x_p$ . For  $x_p \leq 0.5$  only off-resonance data are used. For  $x_p > 0.5$  the weighted average of off-resonance and on-resonance data is used. Fig. 4 is efficiency corrected, and represents the measured fragmentation functions  $D(x)$ , which can be compared to models. The inner error bars show the statistical, the outer error bars the total uncertainties. Fig. 4 is not yet corrected for feed-down from  $D^*$  to  $D^0$ . Details of the feed-down contribution are described elsewhere<sup>7</sup>. The estimated systematic error from  $D^{**}$  feeddown (e.g.  $D_0^*(2308)$  and  $D_1'(2427)$ ) is included and is  $\leq 13\%$ . Tab. 1 shows the functional form of the different fragmentation models which are considered. These are the Peterson<sup>4</sup>, the Kartvelishvili<sup>14</sup> the Collins-Spiller<sup>15</sup> the Lund<sup>16</sup> and the Bowler<sup>17</sup> models. The  $(1-x)$  term in all functional forms originates from the kinematics of radiation of one gluon. For every model a  $\chi^2$  is calculated from the bin-by-bin differences between the model and the data, while the model parameters are optimized in a fit procedure in order to find the optimum values. Fig. 5 shows the measured  $D^{*+}$  fragmentation function in comparison to the models, and Tab. 1 lists the minimum  $\chi^2/d.o.f.$ . The number of the degrees of freedom (*d.o.f.*) is given by the number of  $x_p$  bins minus the free parameters of the fit (one or two, depending upon the model). For the model comparison, the  $D^*$  is chosen instead of the  $D^0$  in order to avoid the feed-down correction. The  $\chi^2$  values for all other hadrons can be found elsewhere<sup>7</sup>. The  $\chi^2$  is not based upon the pure functional form, but instead the MC generated fragmentation function according to the functional form. Thus, the detector resolution, as modeled by GEANT, as well as the parton shower, as modeled by PYTHIA, is taken into account. The models by Collins and Spiller and by Kartvelishvili are not included in the PYTHIA generator. Therefore, a reweighting procedure has been applied. For each event, the  $z$  and the  $p_\perp$  values are stored, and the fragmentation function ansatz is recalculated. Tab. 2 shows the parameters at the minimum  $\chi^2$  of the fit for all different hadrons. The fitted parameters indicate that the PYTHIA default parameters are not well suited for charm fragmentation. As an example, the PYTHIA default for the exponent  $a$  of the  $(1-x)^a$  term in the Lund fragmentation model is  $a=0.30$ , but our fit gives as result  $a=0.68$  at the minimum  $\chi^2$ . However, this is a global PYTHIA parameter, i.e. the parameter is valid for fragmentation of all quark flavors, and for e.g. the light quark sector the parameter might be different from our result. As a result of the comparison, the Bowler and the Lund models appear favored. This is consistent with an observation which was also reported<sup>18</sup> for  $B$  meson fragmentation. The reason might be given by the  $\exp(-bm_\perp^2/z)$  term with the explicit use of the transverse mass  $m_\perp$  which appears in the functional form of these two models, but not in any of the other models.

#### 4. High $x$ region

The measured data were used in a theoretical study<sup>19</sup> in order to investigate possible non-perturbative QCD effects. For this purpose, the fragmentation function is split into a perturbative and a non-perturbative part, i.e.  $D(x)=D_P(x)+D_{NP}(x)$ , with

$$D_{NP} = f_{NP} \cdot \frac{1}{1+c} [\delta(1-x) + c \frac{1}{N_2} (1-x)^a x^b] \quad (1)$$

using the normalisation  $N=\int_0^1(1-x)^a x^b$ . The factor  $f_{NP}$  indicates the relative fraction of the non-perturbative contribution and is determined by a fit. While for the cases of the  $D^*$  mesons the non-perturbative contribution is  $f_{NP}\simeq 21\text{-}25\%$ , for the  $D^0$  meson it turns out to be quite high with  $f_{NP}\simeq 60\%$ . The reason is, that a large fraction of the  $D^0$  mesons arises from  $D^*$  decay. The decay is very close to threshold, and thus the hadron momenta are almost equal, i.e.  $p(D^*)\simeq p(D^0)$ . However, in the decay, a hadronic formfactor transition from a spin 1 hadron (i.e. the  $D^*$ ) to a spin 0 hadron (i.e. the  $D^0$ ) occurs. The partons involved into this transition must be soft, and thus non-perturbative QCD power corrections are expected to occur.

#### 5. Summary

Charm fragmentation functions were measured at  $\sqrt{s}\simeq 10.6$  GeV with high precision. The data were compared to five different fragmentation models, and the model parameters for the best fit to the data were given. The parameters can be used as input for PYTHIA. Among the five models, the Bowler and the Lund model are favoured. The data are posted<sup>20</sup> to the DURHAM reaction database.

#### References

1. Belle Collab., A. Abashian et al., Nucl. Instr. Meth. **A479**, 117 (2002)
2. S. Kurokawa and E. Kikutani, Nucl. Instr. Meth. **A499**, 1 (2003)
3. See <http://www.lns.cornell.edu/public/CLEO/soft/QQ>.
4. C. Peterson, D. Schlatter, I. Schmitt, P. M. Zerwas, Phys. Rev. **D27**, 105 (1983)
5. T. Sjöstrand et al., *Comp. Phys. Comm.* **135**, 238 (2001)
6. R. Brun et al., GEANT 3.21, *CERN Report DD/EE/84-1* (1984)
7. Belle Collab., R. Seuster et al., *Phys. Rev.* **D73**, 032002 (2006)
8. ARGUS Collab., H. Albrecht et al., *Z. Phys.* **C52**, 353 (1991)
9. CLEO Collab., D. Bortoletto et al., *Phys. Rev.* **D37**, 1719 (1988)
10. CLEO Collab., M. Artuso et al., *Phys. Rev.* **D70**, 112001 (2004)
11. CLEO Collab., R. A. Briere et al., *Phys. Rev.* **D62**, 072003 (2000)
12. BABAR Collab., B. Aubert et al., *Phys. Rev.* **D65**, 091104 (2002)
13. S. Eidelman et al., *Phys. Lett.* **B592**, 1 (2004)
14. V. G. Kartvelishvili, A. K. Likhoded, V. A. Petrov, *Phys. Lett.* **B78**, 615 (1978)
15. P. D. B. Collins, T. P. Spiller, *Jour. Phys. G* **11**, 1289 (1985)
16. B. Andersson, G. Gustafson, B. Söderberg, *Z. Phys. C* **20**, 317 (1983)
17. M. G. Bowler, *Z. Phys. C* **11**, 169 (1981)
18. The SLD Collaboration, K. Abe et al., *Phys. Rev.* **D65**, 092006 (2002)
19. M. Cacciari, P. Nason, C. Oleari, *JHEP* **0604**, 006 (2006), hep-ph/0510032
20. See <http://durpdg.dur.ac.uk/cgi-bin/hepdata/testreac/11582/FULL/q>.

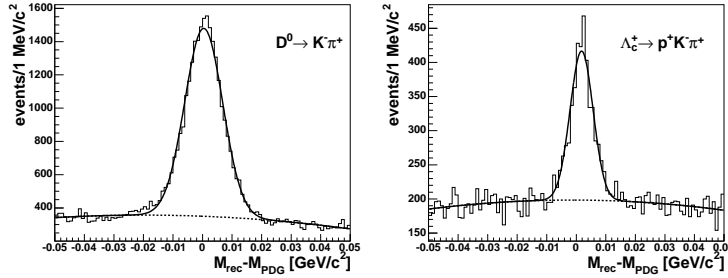
6 *J. S. Lange, Belle Collaboration*


Fig. 2. Mass distributions for the  $D^0$  (left) and the  $\Lambda_c^+$  (right) for a momentum fraction  $0.68 < x_p < 0.70$ . The histograms show the data, the dotted lines describe only the background, the full lines describe the signal and the background.

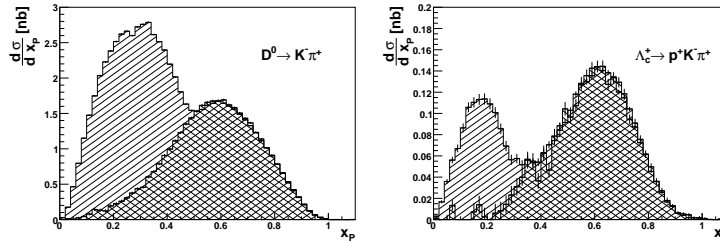


Fig. 3. The cross section  $d\sigma/dx_p$  as a function of  $x_p$  for  $D^0$  (left) and  $\Lambda_c^+$  (right). The down-left hatched histogram shows on-resonance data, the down-right hatched histogram off-resonance data.

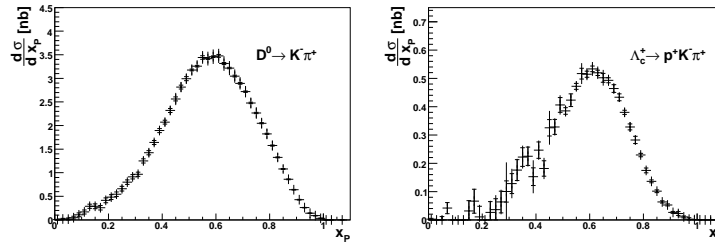


Fig. 4. Efficiency corrected cross section  $d\sigma/dx_p$  as a function of  $x_p$ . For  $x_p \leq 0.5$  only off-resonance data are used. For  $x_p > 0.5$  the weighted average of off-resonance and on-resonance data is used.

Table 1. Functional form of the fragmentation functions used in this analysis. The normalisation  $N$  is different for all functions. In the last column, the  $\chi^2/\text{d.o.f.}$  from the comparison to the data for the case of the  $D^{*+}$  (see Fig. 5) is shown as an example.

Model	Functional Form	$\chi^2/\text{d.o.f.}$ for $D^{*+}$
Bowler	$N \frac{1}{z^{1+bm^2}} (1-z)^a \exp\left(-\frac{bm^2}{z}\right)$	541.8 / 55
Lund	$N \frac{1}{z} (1-z)^a \exp\left(-\frac{bm^2}{z}\right)$	965.6 / 55
Kartvelishvili	$N z^{\alpha_c} (1-z)$	1271.1 / 54
Collins-Spiller	$N \left( \frac{1-z}{z} + \frac{(2-z)\epsilon'_c}{1-z} \right) (1+z^2) \left( 1 - \frac{1}{z} - \frac{\epsilon'_c}{1-z} \right)^{-2}$	1540.7 / 54
Peterson	$N \frac{1}{z} \left( 1 - \frac{1}{z} - \frac{\epsilon_c}{1-z} \right)^{-2}$	3003.0 / 54

## Charmed Hadrons from Fragmentation and B Decays 7

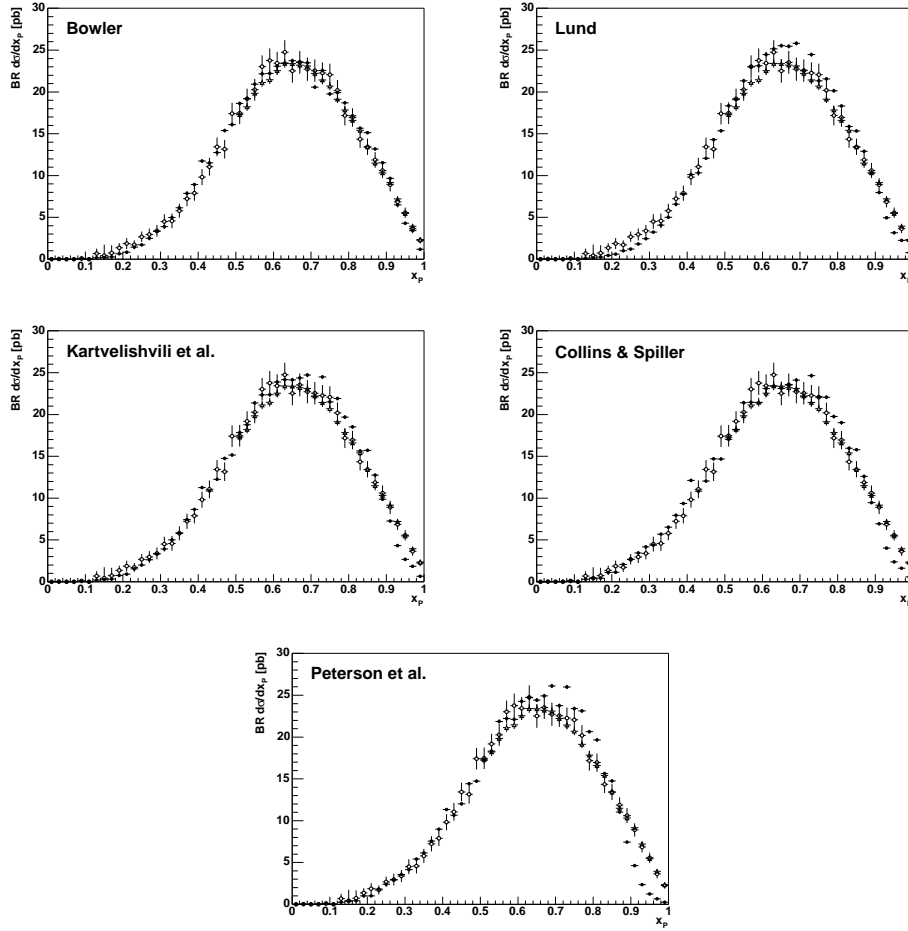


Fig. 5. Efficiency corrected cross section  $BR \times d\sigma/dx_p$  as a function of  $x_p$  in comparison to fragmentation models for  $D^{*+}$  fragmentation (black circles: MC, white circles: on-resonance data, white triangles: off-resonance data). Only statistical errors are shown. The parameters  $a, b$  of the models are optimized by a fit procedure in order to find the best agreement between data and model. The deviations in the  $x \simeq 1$  region are an indication for non-perturbative contributions.

Table 2. The parameters of the fragmentation functions at the minimum of the  $\chi^2/d.o.f.$  distributions, which can be used as input to PYTHIA.

		$D^0$	$D^+$	$D_s^+$	$\Lambda_c^+$	$D^{*+}$
Bowler	$a b$	0.12   0.74	0.12   0.58	0.12   0.68	0.34   0.74	0.22   0.56
Lund	$a$	0.26	0.45	0.2	0.55	0.58
Collins and Spiller	$\varepsilon'_c$	0.04	0.055	0.04	0.04	0.075
Kartvelishvili	$\alpha_c$	4.6	4	5.6	3.6	5.6
Peterson	$\varepsilon_c$	0.028	0.039	0.008	0.011	0.054